



May 2002

# Effect of Seeding on the Microstructure and Mechanical Properties of alpha-SiAlON: I, Y-SiAlON

Misha Zenotchkine  
*University of Pennsylvania*

Roman Shuba  
*University of Pennsylvania, rshuba@seas.upenn.edu*

Joo-Sun Kim  
*University of Pennsylvania*

I-Wei Chen  
*University of Pennsylvania, iweichen@seas.upenn.edu*

Follow this and additional works at: [http://repository.upenn.edu/mse\\_papers](http://repository.upenn.edu/mse_papers)

---

## Recommended Citation

Zenotchkine, M., Shuba, R., Kim, J., & Chen, I. (2002). Effect of Seeding on the Microstructure and Mechanical Properties of alpha-SiAlON: I, Y-SiAlON. Retrieved from [http://repository.upenn.edu/mse\\_papers/35](http://repository.upenn.edu/mse_papers/35)

Copyright The American Ceramic Society. Reprinted from *Journal of the American Ceramic Society*, Volume 85, Issue 5, May 2002, pages 1254-1259.

This paper is posted at ScholarlyCommons. [http://repository.upenn.edu/mse\\_papers/35](http://repository.upenn.edu/mse_papers/35)  
For more information, please contact [libraryrepository@pobox.upenn.edu](mailto:libraryrepository@pobox.upenn.edu).

---

# Effect of Seeding on the Microstructure and Mechanical Properties of $\alpha$ -SiAlON: I, Y-SiAlON

## **Abstract**

The effect of seeding on the microstructure and mechanical properties of single-phase Y- $\alpha$ -SiAlON ceramics with elongated grains has been studied. Seeds of the intended  $\alpha$ -SiAlON compositions but with different size, shape, and number of grains have been compared for their effects. The microstructure, resistance (R-curve) behavior, and Weibull modulus are strongly correlated to the number density of the seeds. The highest fracture toughness reached is  $\sim 12 \text{ MPa}\cdot\text{m}^{1/2}$  and can be obtained with as little as 1% seeding. The thermodynamic stability of seeds has been examined and is attributed to their chemical composition.

## **Comments**

Copyright The American Ceramic Society. Reprinted from *Journal of the American Ceramic Society*, Volume 85, Issue 5, May 2002, pages 1254-1259.

# Effect of Seeding on the Microstructure and Mechanical Properties of $\alpha$ -SiAlON: I, Y-SiAlON

Misha Zenotchkine, Roman Shuba, Joo-Sun Kim, and I-Wei Chen\*

Department of Materials Science and Engineering, University of Pennsylvania, Philadelphia, Pennsylvania 19104-6272

**The effect of seeding on the microstructure and mechanical properties of single-phase Y- $\alpha$ -SiAlON ceramics with elongated grains has been studied. Seeds of the intended  $\alpha$ -SiAlON compositions but with different size, shape, and number of grains have been compared for their effects. The microstructure, resistance (R-curve) behavior, and Weibull modulus are strongly correlated to the number density of the seeds. The highest fracture toughness reached is  $\sim 12 \text{ MPa}\cdot\text{m}^{1/2}$  and can be obtained with as little as 1% seeding. The thermodynamic stability of seeds has been examined and is attributed to their chemical composition.**

## I. Introduction

SILICON nitride solid solution of the  $\alpha$ - $\text{Si}_3\text{N}_4$  structure ( $\alpha$ -SiAlON) is an attractive ceramic because of the combination of high hardness and high toughness.<sup>1–7</sup> Compared with ceramics based on  $\beta$ - $\text{Si}_3\text{N}_4$ , which also has high toughness but a lower hardness, the microstructure of  $\alpha$ -SiAlON is more sensitive to the composition, the processing conditions, and the starting powders.<sup>1–4</sup> As a result, only recently have  $\alpha$ -SiAlON ceramics with elongated grains that enable *in situ* toughening been developed. In view of the complexity of microstructure control, seeding seems to offer an attractive solution because it can effect templated growth of elongated grains. Several reports on seeding in  $\beta$ - $\text{Si}_3\text{N}_4$  based ceramics<sup>8–12</sup> clearly demonstrated the great potential of this method in silicon nitride ceramics. Preliminary efforts for seeding  $\alpha$ -SiAlON using pulverized ceramic fragments as seeds have also been reported.<sup>2,13</sup> Most recently, we reported the growth of single crystal seeds from liquid,<sup>14</sup> and observed a dramatic effect on the enhanced resistance (R-curve) behavior of yttrium- and calcium-containing  $\alpha$ -SiAlON ceramics.<sup>15</sup> Here we have systematically examined the effect of the size, morphology, and number density of seeds on the microstructure and mechanical properties of  $\alpha$ -SiAlON ceramics. The results of yttrium-containing SiAlON are reported here and those of calcium-containing SiAlON are reported in a companion paper.<sup>16</sup>

## II. Experimental Procedures

### (1) Composition

The composition investigated here lies in the center of the single-phase region of the Y- $\alpha$ -SiAlON and is represented by the formula  $\text{Y}_{0.5}\text{Si}_{9.3}\text{Al}_{9.3}\text{O}_{1.2}\text{N}_{14.8}$ . This has been referred to as Y-1512 in our previous studies.<sup>2,14,15</sup> The notation indicates  $m =$

1.5 and  $n = 1.2$  in the conventional designation of  $\alpha$ -SiAlON,  $\text{M}_{m/z}\text{Si}_{12-(m+n)}\text{Al}_{(m+n)}\text{O}_n\text{N}_{(16-n)}$ , in which M stands for an interstitial cation of a valence ( $z$ ). This composition is known to be rather stable and can be prepared using  $\text{Si}_3\text{N}_4$ , AlN,  $\text{Y}_2\text{O}_3$ , and  $\text{Al}_2\text{O}_3$ , as shown in Table I.

### (2) Seed Crystals

Y- $\alpha$ -SiAlON seed crystals of Y-1512 composition were prepared using the method described elsewhere.<sup>14</sup> Briefly, these crystals were grown from a liquid that was contained in a powder mixture of various appropriate compositions and fired at  $1700^\circ\text{C}$  in a nitrogen atmosphere. Seed crystals were harvested by separating them from the mixture using a procedure involving mechanical separation and chemical treatment. X-ray powder diffraction was used to verify that these crystals were single-phase  $\alpha$ -SiAlON with lattice parameters that were essentially the same as those of Y-1512 ceramic. The size (width and length) and morphology (aspect ratio) of seed crystals were analyzed for more than 200 crystals using micrographs obtained from scanning electron microscopy (SEM).

### (3) Powder and Ceramic Preparation

Starting powders of  $\alpha$ - $\text{Si}_3\text{N}_4$  (SN-E-10, UBE Industries, Yamaguchi, Japan), AlN (type F, Tokuyama Soda Co., Menlo Park, CA),  $\text{Al}_2\text{O}_3$  (AKP50, Sumitomo Chemical America, New York), and  $\text{Y}_2\text{O}_3$  (P3598, Alfa Aesar/Johnson Matthey Co., Ward Hill, MA) were used to prepare Y-1512 ceramics (see powder composition in Table I). The residual oxygen content in  $\alpha$ - $\text{Si}_3\text{N}_4$  and AlN were considered in the formulation. Powder mixtures were attrition milled in isopropyl alcohol for 2 h with high-purity  $\text{Si}_3\text{N}_4$  milling media in a Teflon-coated jar. Charges of seed crystals of a certain weight percent were then added and milled for an additional 10–15 min. Powder slurries were subsequently dried in a polyethylene beaker under a halogen lamp while being stirred. Charges of 20 g of powders were hot pressed in a graphite resistance furnace at  $1900^\circ\text{C}$  for 1 h in a nitrogen atmosphere, under a uniaxial pressure of 30 MPa. Full densification was achieved in all experiments. The phase purity and the composition were assessed using X-ray diffraction (XRD) by comparing peak positions with the published data of lattice parameters.<sup>17</sup> In all cases, the pulverized powders of the ceramics revealed the single-phase diffraction pattern of  $\alpha$ -SiAlON with the lattice parameters given in Table I. These parameters are essentially the same as those of other Y-1512 ceramics reported in the literature.

### (4) Ceramic Characterization

Microstructures of ceramic samples were observed on polished sections after etching in boiling solution of 20 g  $\text{NH}_4\text{F}$  in 50 mL  $\text{HNO}_3$ .<sup>18</sup> SEM and optical microscopy were used for microstructure observations. Statistical data of the microstructure were collected on the cross section normal to the hot-pressing axis. Vickers hardness and indentation fracture toughness<sup>19</sup> were obtained at 10 kg load. (Shimadzu-HSV-20, Shimadzu Corp., Kyoto, Japan). R-curve was measured in four-point bending. Bars of 30 mm  $\times$  4 mm  $\times$  2 mm, with their tensile surface lying parallel to

P. F. Becher—contributing editor

Manuscript No. 187584. Received July 16, 2001; approved February 7, 2002. Supported by the U.S. Air Force Office of Scientific Research, under Grant No. F49620-01-1-0150. Facilities at the University of Pennsylvania are supported by the U.S. National Science Foundation under MRSEC Grant No. DMR00-79909.  
\*Member, American Ceramic Society.

**Table I. Composition and Lattice Parameters of Y-1512 Ceramics**

Parameter	Value
Composition of starting powder	
Si <sub>3</sub> N <sub>4</sub> (1.24% oxygen)	72.25
AlN (0.88% oxygen)	18.12
Al <sub>2</sub> O <sub>3</sub>	0.29
Y <sub>2</sub> O <sub>3</sub>	9.33
Lattice parameters of ceramics	
<i>a</i> (Å)	7.827 (1)
<i>c</i> (Å)	5.705 (1)

the hot-press plane, were used. The initial crack of  $\sim 0.1$ – $0.2$  mm long was introduced using a thin blade followed by wire sawing to achieve a tip radius of  $10\ \mu\text{m}$ . Crack length was measured *in situ* under a microscope with a resolution of  $2$ – $5\ \mu\text{m}$ . Further details of this procedure are available elsewhere.<sup>15</sup>

Strength was measured in three-point bending using samples of a dimension  $30\ \text{mm} \times 4\ \text{mm} \times 1\ \text{mm}$ . An outer span of  $13\ \text{mm}$  and a crosshead speed of  $0.5\ \text{mm/min}$  were used. Samples were mounted in silicon carbide or silicon nitride fixtures and loaded in a digitally controlled servohydraulic testing machine (MTS-810, MTS Systems Corp., Minneapolis, MN). Strength was calculated from the following formula:

$$\sigma = \frac{3P_{\max}^s}{2bw^2}$$

Here  $P_{\max}$  is the maximum load at fracture,  $s$  is the span,  $b$  is the width, and  $h$  is the height of the bend bar.

### III. Results

#### (1) Seed Crystals

Three types of Y-1512 seed crystals were used to compare their effect on the microstructure and properties of the seeded ceramics. These included two types of elongated seed crystals, denoted as S-1 and S-2 (Figs. 1(a) and (b)) and one equiaxed type, denoted as S-3 (Fig. 1(c)). As shown in Fig. 1 and Table II, S-1 and S-2 have very similar aspect ratios (AR), but S-2 is nearly twice as large in area as S-1. This means that, at the same weight, the areal number density of S-1 is twice that of S-2. The equiaxed type, S-3, has nearly the same area as S-1. These seeds have essentially the same composition. (See Table II for lattice parameters of seeds. These values are essentially the same as the ones for the ceramics of the overall composition,  $m = 1.5$  and  $n = 1.2$ ; see lattice parameters given in Table I). Therefore, a comparison of the seeding effect of S-1 and S-2 would reveal the influence of crystal size, whereas a similar comparison of S-1 and S-3 would reveal the influence of aspect ratio.

#### (2) Microstructure

Microstructures of unseeded and some seeded ceramics are shown in Fig. 2. Unseeded ceramic (Fig. 2(a)) contains mostly small and equiaxed grains; large grains are relatively few and not always elongated. Seeding at 1% led to the formation of many large elongated grains (Fig. 2(b)–(c)). The microstructures are rather similar no matter whether elongated (S-1, Fig. 2(b)) or equiaxed (S-3, Fig. 2(c)) seeds were used. The largest numbers of highly elongated grains were observed in samples with 1%–2% of seeds. With a further increase of the seed amount, both grain size and AR tend to decrease, indicating a mutual hindrance effect among seeds (Fig. 2(d) where 5% of S-2 was used). In addition, porosity was observed in some samples at 5% seeding. Qualitatively similar microstructures (not shown) were also obtained using the larger (S-2) seeds.

To ascertain that the aspect ratio of seeds is not an important parameter for microstructure development, we have quantitatively compared the statistics of elongated grains in Figs. 2(b) and (c).

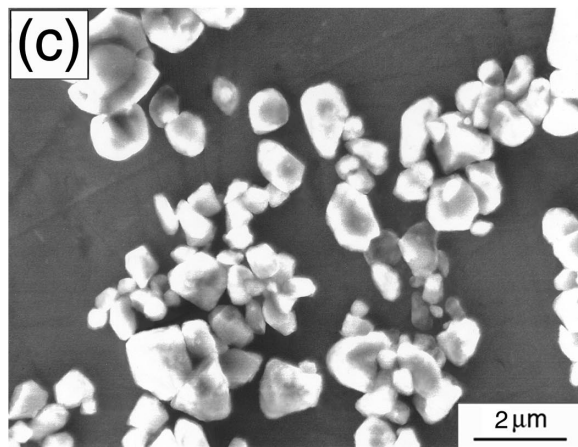
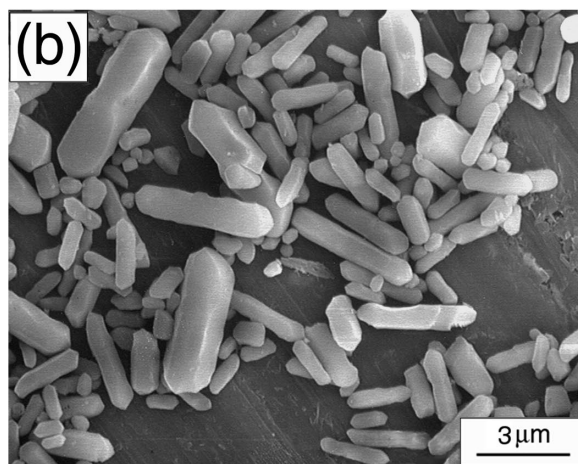
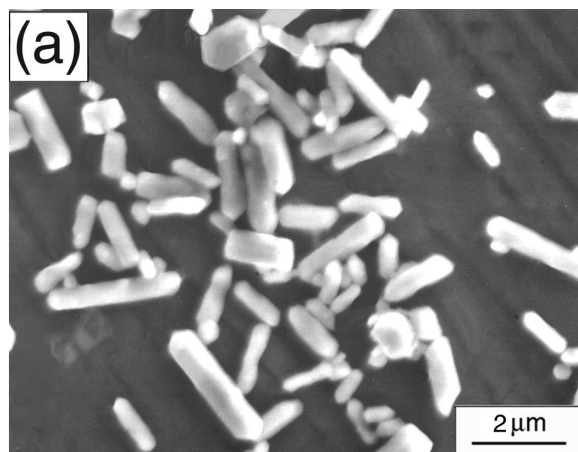


**Fig. 1.** SEM micrographs of (a), (b) elongated and (c) equiaxed seed crystals. They correspond to S-1, S-2, and S-3, respectively, in Table II.

For this analysis, we included all the grains with a width ( $W$ ) larger than  $1\ \mu\text{m}$ , and measured their width and length ( $L$ ) to compute the AR and grain area ( $A = WL$ ). More than 650 grains were taken into account in this analysis for each sample. As shown in Table III, the average measures for the two microstructures are quite similar. This is also true with their distributions. For example, Fig. 3 shows very similar grain length distributions in the two microstructures.

#### (3) Core-Shell Microstructure

Direct evidence for the presence of seed crystals in the final ceramics was found in the above microstructures. A close view of large, elongated grains in Figs. 2(b)–(d) clearly shows small

**Table II. Lattice Parameters and Average Dimensions of Seed Crystals**

Parameter	Value		
	S-1 (Small elongated)	S-2 (Large elongated)	S-3 (Equiaxed)
Lattice parameters			
<i>a</i> (Å)	7.827 (2)	7.829 (2)	7.830 (2)
<i>c</i> (Å)	5.705 (2)	5.705 (2)	5.705 (2)
Average dimensions			
<i>W</i> (μm)	0.36 ± 0.09	0.54 ± 0.29	0.55 ± 0.26
<i>L</i> (μm)	1.06 ± 0.49	1.39 ± 0.85	0.77 ± 0.39
AR	2.52 ± 1.02	2.48 ± 1.03	1.40 ± 0.31
<i>A</i> (μm <sup>2</sup> )	0.38	0.75	0.42

“cores,” marked by arrows in Figs. 2(b) and (c), in the centers of large grains. These cores retain the shape of the original seeds, elongated in the case of S-1 (Fig. 2(b)) and equiaxed in the case of S-3 (Fig. 2(c)). This indicates that large elongated grains were grown from the seed crystals.

Another direct evidence of the heterogeneous nature of crystallization of α-SiAlON onto seed crystals was provided by the following model experiment. A Yb-α-SiAlON (Yb-1512) ceramic was prepared with 1% S-2 seeds (Y-1512) following the same procedure as described earlier, giving the microstructure shown in Fig. 4. Because the atomic number of ytterbium (70) is much

**Table III. Microstructure Characteristics of Two Seeded Y-α-SiAlON Ceramics**

Parameter	Value	
	Y-1512 + 1% elongated S-1 seeds	Y-1512 + 1% equiaxed S-3 seeds
<i>W</i> (μm)	1.85 ± 0.50	1.74 ± 0.49
<i>L</i> (μm)	4.34 ± 2.39	3.82 ± 2.05
<i>A</i> (μm <sup>2</sup> )	8.03	6.64
AR	2.32 ± 1.01	2.18 ± 0.93

higher than that of yttrium (39), the back-scattering-electron contrast between yttrium and ytterbium reveals in Fig. 4 dark cores of Y-α-SiAlON seed crystals in the centers of bright Yb-α-SiAlON grains.

#### (4) R-curve

Fracture R-curves obtained for unseeded and seeded ceramics are shown in Fig. 5. Compared with the unseeded ceramic, seeded ceramics have much higher fracture toughness in all cases. The highest toughness achieved is between 10 and 12 MPa·m.<sup>1/2</sup> Note that the toughness increase is not a monotonic function of the amount of seed. This is best illustrated in Fig. 6, which plots the values of peak toughness (taken at a crack length of 1200 μm) and minimum toughness on the R-curve as a function of seed content. They suggest that S-1 and S-3 seeds have a similar effect, in that

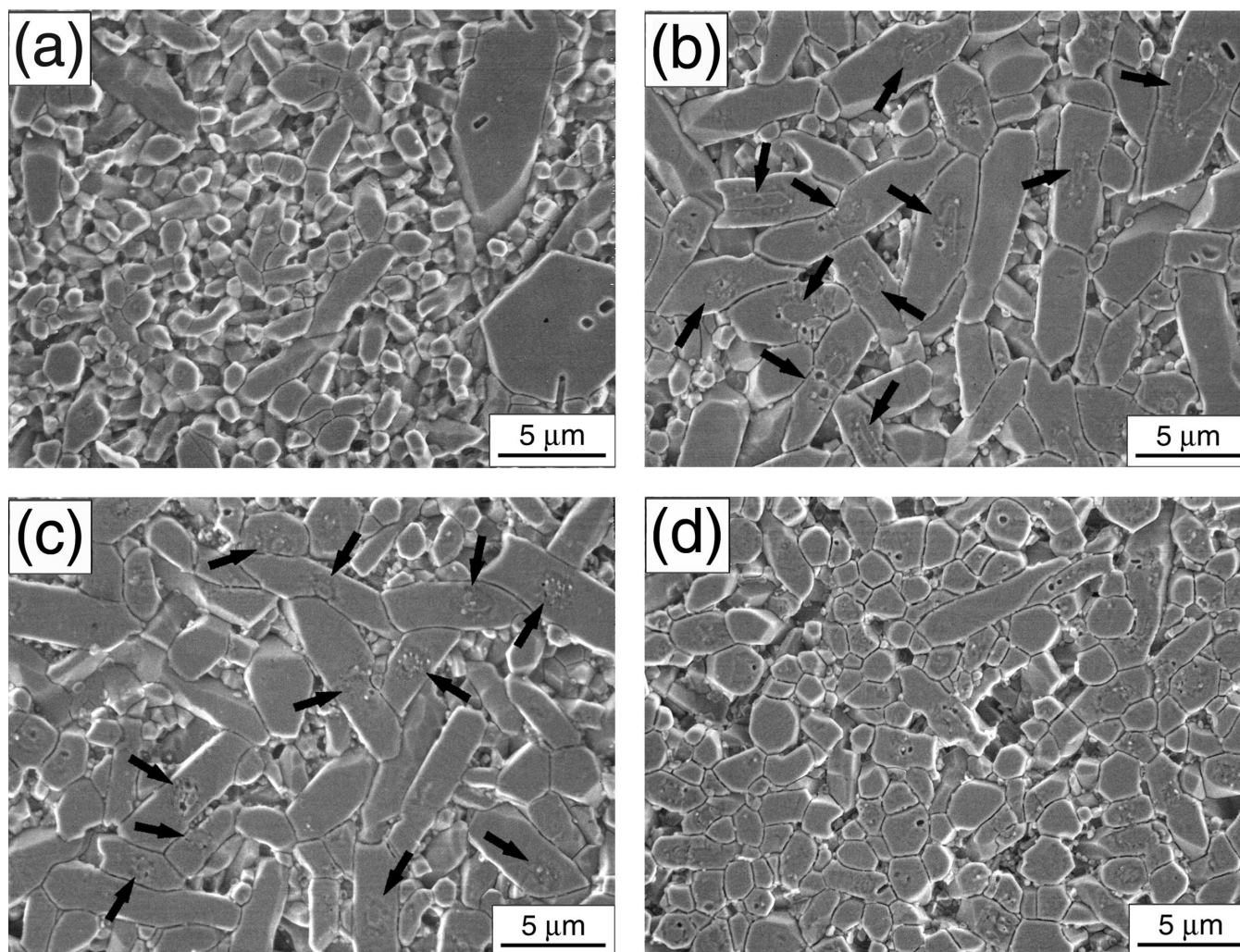


**Fig. 2.** SEM micrographs of Y1512 ceramics; (a) unseeded, (b) seeded by 1% elongated S-1 seeds, (c) seeded by 1% equiaxed S-3 seeds, and (d) seeded by 5% elongated S-1 seeds. Arrows indicate core-shell microstructures.

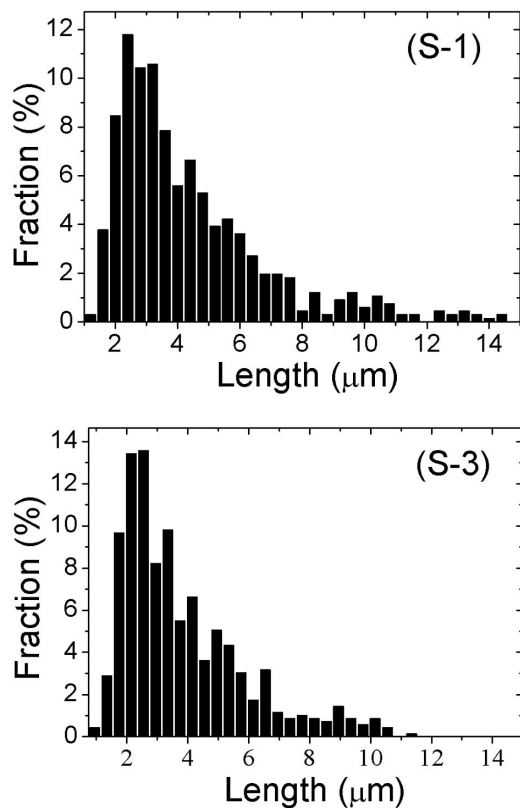


Fig. 3. Length distributions of large grains (width over 1  $\mu\text{m}$ ) in ceramics with 1% seeding of elongated (S-1) seeds and equiaxed (S-3) seeds.

the peak toughening is achieved at  $\sim 1\%$  of seeding. This observation is consistent with their effects on the microstructure, which are also similar. Ceramics seeded by S-2 reach peak toughening at a higher seed content,  $\sim 2\%$ . This may be related to the fact that, at the same weight percent, the areal number density of S-2 seeds is nearly half of that for S-1 and S-3 seeds.

#### (5) Indentation Toughness and Hardness

Data of indentation toughness are also shown in Fig. 6. While it underestimates the peak toughness because of the short crack length generated by the indent, the indentation toughness, perhaps fortuitously, follows the same trend as peak R-curve toughness shown in the same figure. In our previous work, we have used pulverized fragments of  $\alpha$ -SiAlON ceramics as seeds.<sup>2</sup> These fragments ranged from 1–3  $\mu\text{m}$  in size, and the “cores” observed in the final ceramic microstructure were of the same size. The data of indentation toughness of those samples showed a peak at 5% seed content, with a toughness value of 4.8  $\text{MPa}\cdot\text{m}^{1/2}$ .<sup>2</sup> Comparing these data, we can state that the smaller single crystal seeds are more effective because a smaller amount of them is needed to achieve peak toughening.

Vickers indentation hardness measured at 10 kg load was  $\sim 21$  GPa for this series of ceramics. This suggests that the hardness is independent of the microstructure, which is a common observation for ceramics.<sup>20,21</sup>

#### (6) Strength and Weibull Modulus

Preliminary bend strength data of unseeded and seeded ceramics (using S-2 seeds) are  $\sim 800$  MPa. A small increase of strength with the amount of seed was observed, although at 5% seeding the strength deteriorated slightly because of increasing porosity. The Weibull modulus for each microstructure was calculated from strength distributions (Fig. 7). The results illustrate a significant improvement of the reliability of ceramics with coarse elongated microstructure, which is similar to the reported results for  $\beta$ - $\text{Si}_3\text{N}_4$

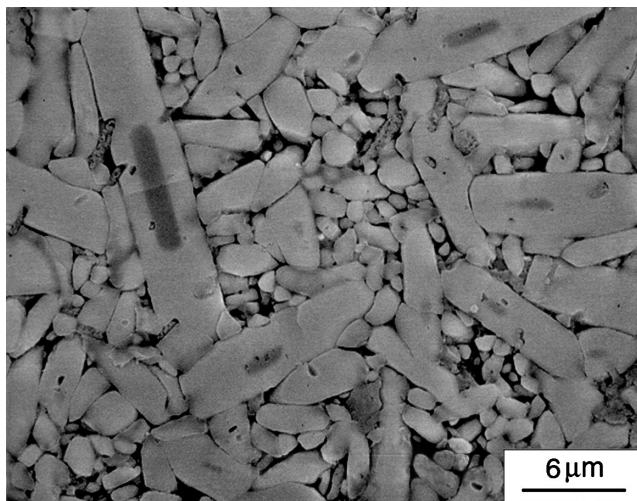


Fig. 4. SEM micrograph of Yb-SiAlON showing elongated grains grown around Y-SiAlON seeds (dark).

ceramics.<sup>22</sup> Further investigation of the strength-microstructure relationship is under way and will be reported in the future.

## IV. Discussion

The present study reaffirms the utility of seeding as a means for microstructure control in silicon nitride ceramics. Seeding allows templated growth of elongated grains and is most effective when the concentration of seeds is optimized to maximize the concentration of elongated grains in the final microstructure. This optimization depends on the number of initial seed crystals that survive processing and serve as the nucleation sites for  $\alpha$ -SiAlON precipitation during liquid-phase sintering. As this number increases, more elongated grains should be found until they impinge on each other. Following this thinking, we suggest that the single crystal seeds used in this study are more effective than the ceramic fragments used in our previous work, because the latter are larger in size ( $W$  from 1–3  $\mu\text{m}$ ). As a result, more weight percentage of fragments than that for single crystal seeds is needed to achieve the same number density. The fact that large single crystals (S-2) are less effective than small single crystals (S-1) also supports this notion: the number density of seeds is important for microstructure control. Indeed, both equiaxed (S-3) and elongated (S-1) crystals, which have the same cross-sectional area on average, are about equally effective in producing the desired microstructure and in achieving peak fracture toughness.

The above results can be rationalized if we assume that all the seed crystals used here are thermodynamically stable, that none dissolves during liquid-phase sintering, and that every one of them is an effective nucleation site for  $\alpha$ -SiAlON precipitation. This hypothesis is difficult to prove given the complicated phase and microstructure evolution in forming the final  $\alpha$ -SiAlON ceramics, but it seems to be supported by the following crude estimation. From the average dimensions of seeds in Table II and the average dimensions of elongated grains in Table III, we can calculate the average volume,  $V = W^2L$ , for the seeds and the grains. The ratio of such volumes is  $\sim 100$  for S-1 seeding and  $\sim 50$  for S-3 seeding. Because the ceramics in Table III contain 1% seeds, a one-to-one correspondence between the seed crystal in the starting powders and the large elongated grain in the final ceramic would yield a ratio of 100, which is of the same order of magnitude as observed. This suggests that a large fraction, if not all, of seed is an effective nucleation site for  $\alpha$ -SiAlON precipitation.

To survive liquid-phase sintering, seed crystals must be thermodynamically stable compared with other particles in the starting powders. Stabilization can be attributed to either a size advantage or a chemical advantage. Large crystals are more stable because of

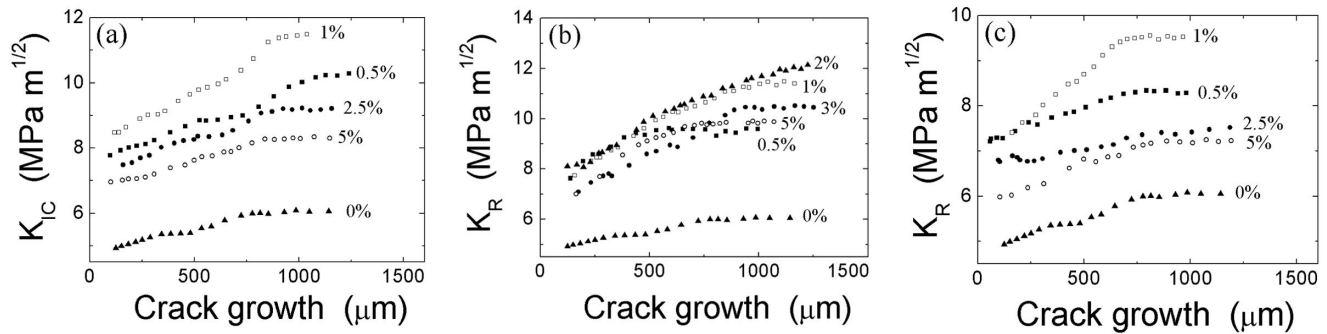


Fig. 5. R-curves of Y1512 ceramics seeded by different amounts of (a) S-1, (b) S-2, and (c) S-3 seeds.

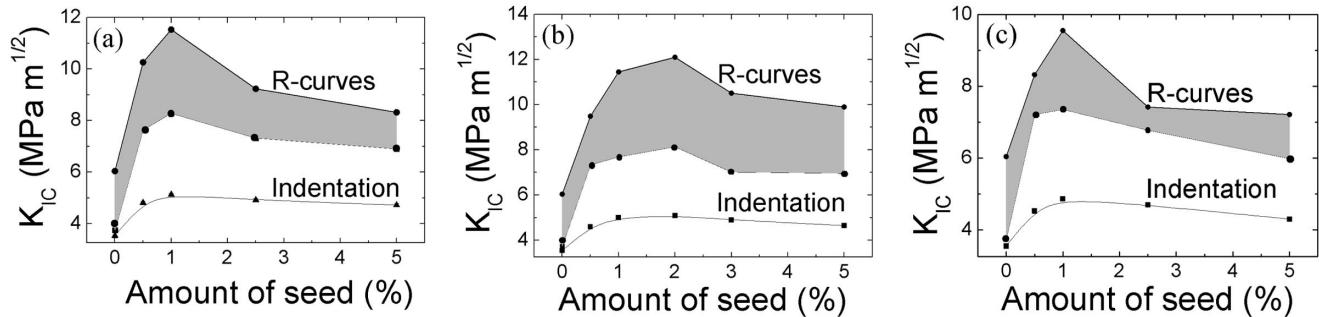


Fig. 6. Peak and initial fracture toughness on R-curves for Y1512 ceramics seeded by different amounts of (a) S-1, (b) S-2, and (c) S-3 seeds. Indentation toughness also shown.

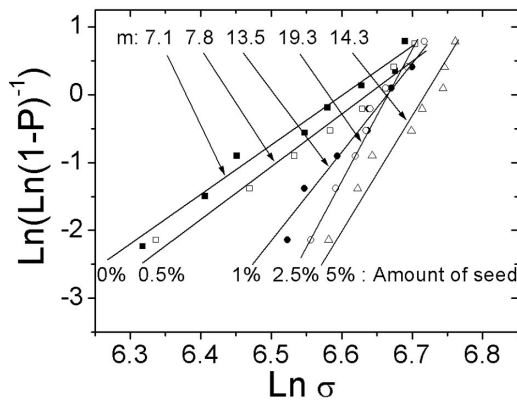


Fig. 7. Strength distribution as function of amount of S-2 seeds for Y1512 ceramics.

a smaller surface tension. For a rod-like silicon nitride crystal that is not necessarily at equilibrium, the chemical potential is difficult to estimate for the side surface where interface control may cause deviations from thermal equilibrium.<sup>23</sup> However, the chemical potential at the end surface, which is usually atomically rough, can be evaluated by computing the increase of the (side) surface energy when the end grows by one atomic layer. The chemical potential thus evaluated is independent of the length of the crystal but is related to its radius by  $2\gamma\Omega/R$ .<sup>24</sup> Here  $\gamma$  is the interfacial energy per unit area of the side surface,  $\Omega$  is the atomic volume, and  $R$  is the radius of the rod (taken to be  $W/2$ ). In the present study, the width of our seed crystals is  $\sim 0.5 \mu\text{m}$ , and the width of the starting (equiaxed and mostly  $\alpha\text{-Si}_3\text{N}_4$ ) powders is from 0.5–1.5  $\mu\text{m}$  according to the manufacturer. Thus, the width of the seed crystals is roughly comparable to that of the starting powders and offers no special size advantage. So the reason that our seeds are effective must be attributed to their chemical stability. This is plausible because our seeds have the intended composition and

structure of Y-1512  $\alpha\text{-SiAlON}$ , whereas the starting  $\alpha\text{-Si}_3\text{N}_4$  powders are unstable at this overall composition. (The dissolution of  $\alpha\text{-Si}_3\text{N}_4$  before  $\alpha\text{-SiAlON}$  formation was documented by XRD study by Rosenflanz and Chen.<sup>25</sup>)

The fact that both elongated and equiaxed seeds are nearly equally effective suggests that their thermodynamic stability is similar as a result of their similar chemical compositions. The small difference between their seeding effectiveness (e.g., the different ratio of grain volume to seed volume in the microstructure) may be caused by the larger width of the S-3 seeds (0.55  $\mu\text{m}$  on average) compared with the S-1 seeds (0.36  $\mu\text{m}$  on average). This will make the latter seeds less stable, which may cause some smaller S-1 seeds to dissolve and the remaining ones to grow further with less competition.

## V. Conclusions

(1) Single crystal seeds of  $\alpha\text{-SiAlON}$  compositions have been used for microstructure control of *in situ* toughened  $\alpha\text{-SiAlON}$ . As little as 1% seeding is sufficient to yield high-toughness ceramics, with a peak toughness reaching  $12 \text{ MPa m}^{1/2}$  with improved strength and Weibull modulus.

(2) Seed crystals of  $\alpha\text{-SiAlON}$  composition are more stable than starting powders even though their sizes are comparable. During liquid-phase sintering, a large fraction of seed crystals survives and provides the sites for  $\alpha\text{-SiAlON}$  precipitation.

(3) The number density of stable seed crystals is the dominant factor for microstructure control, regardless of the shape and size of the crystals.

## References

1. I.-W. Chen and A. Rosenflanz, "A Tough SiAlON Ceramic Based on  $\alpha\text{-Si}_3\text{N}_4$  with a Whisker-like Microstructure," *Nature*, **389**, 701–704 (1997).
2. J. Kim, A. Rosenflanz, and I.-W. Chen, "Microstructure Control of *in situ* Toughened  $\alpha\text{-SiAlON}$  Ceramics," *J. Am. Ceram. Soc.*, **83** [7] 1819–21 (2000).
3. A. Rosenflanz and I.-W. Chen, "Phase Relationships and Stability of  $\alpha\text{-SiAlON}$ ," *J. Am. Ceram. Soc.*, **82** [4] 1025–36 (1999).

- <sup>4</sup>W. W. Chen, W. Y. Sun, Y. W. Li, and D. S. Yan, "Effect of Processing on the Morphology of  $\alpha$ -SiAlON Grains," *Mater. Lett.*, **46** [6] 343–48 (2000).
- <sup>5</sup>P. L. Wang, C. Zhang, W. Y. Sun, and D. S. Yan, "Characteristics of Ca- $\alpha$ -sialon-Phase Formation, Microstructure and Mechanical Properties," *J. Eur. Ceram. Soc.* **19** [5] 553–60 (1999).
- <sup>6</sup>H. Mandal and M. J. Hoffmann, "Hard and Tough  $\alpha'$ -SiAlON Ceramics," *Mater. Sci. Forum.*, **325** [3] 219–24 (2000).
- <sup>7</sup>C. A. Wood, H. Zhao, and Y.-B. Cheng, "Microstructural Development of Ca Alpha-SiAlON Ceramics with Elongated Grains," *J. Am. Ceram. Soc.*, **82**, 421–28 (1999).
- <sup>8</sup>K. Hirao, T. Nagaoka, M. E. Brito, and S. Kanzaki, "Microstructure Control of Silicon Nitride by Seeding with Rodlike  $\beta$ -silicon Nitride Particles," *J. Am. Ceram. Soc.*, **77** [7] 1857–62 (1994).
- <sup>9</sup>H. Imamura, K. Hirao, M. E. Brito, M. Toriyama, and S. Kanzaki, "Further Improvement in Mechanical Properties of Highly Anisotropic Silicon Nitride Ceramics," *J. Am. Ceram. Soc.*, **83** [3] 495–500 (2000).
- <sup>10</sup>P. D. Ramesh, R. Oberracker, and M. J. Hoffmann, "Preparation of  $\beta$ -Silicon Nitride Seeds for Self-reinforced Silicon Nitride Ceramics," *J. Am. Ceram. Soc.*, **82** [6] 1608–10 (1999).
- <sup>11</sup>M. Kitayama, K. Hirao, M. Toriyama, and S. Kanzaki, "Control of  $\beta$ -Si<sub>3</sub>N<sub>4</sub> Crystal Morphology and Its Mechanism: Part 1, Effect of SiO<sub>2</sub> and Y<sub>2</sub>O<sub>3</sub> Ratio," *J. Ceram. Soc. Jpn.*, **107** [10] 930–34 (1999).
- <sup>12</sup>S. Y. Lee, K. A. Appiagyei, and H. D. Kim, "Effect of  $\beta$ -Si<sub>3</sub>N<sub>4</sub> Seed Crystal on the Microstructure and Mechanical Properties of Sintered Reaction Bonded Silicon Nitride," *J. Mater. Res.*, **14** [1] 178–84 (1999).
- <sup>13</sup>W. W. Chen, W. Y. Sun, Y. W. Li, and D. S. Yan, "Microstructure of (Y+Sm)-alpha-SiAlON with Alpha-SiAlON Seeds," *J. Mater. Res.*, **15** [10] 2223–27 (2000).
- <sup>14</sup>M. Zenotchkine, R. Shuba, J.-S. Kim, and I.-W. Chen, "Synthesis of  $\alpha$ -SiAlON Seed Crystals," *J. Am. Ceram. Soc.*, **84** [7] 1651–53 (2001).
- <sup>15</sup>M. Zenotchkine, R. Shuba, J.-S. Kim, and I.-W. Chen, "R-Curve Behavior of In-situ Toughened  $\alpha$ -SiAlON Ceramics," *J. Am. Ceram. Soc.*, **84** [4] 884–86 (2001).
- <sup>16</sup>R. Shuba and I.-W. Chen, "Effect of Seeding on the Microstructure and Mechanical Properties of  $\alpha$ -SiAlON, II. Ca-SiAlON," *J. Am. Ceram. Soc.*, **85** [5] 1260–67 (2002).
- <sup>17</sup>W.-Y. Sun, T.-Y. Tien, and T.-S. Yen, "Solubility Limits of  $\alpha$ -SiAlON Solid Solutions in the System Si<sub>3</sub>Al<sub>2</sub>Y/N<sub>2</sub>O," *J. Am. Ceram. Soc.*, **74** [10] 2547–50 (1991).
- <sup>18</sup>A. I. Mamchik, J. S. Kim, and I.-W. Chen, "A New Method for Etching Silicon Nitride Ceramics"; p. 191, abstract of 101st Annual Meeting & Exposition of American Ceramic Society (1999).
- <sup>19</sup>G. R. Anstis, P. Chantikul, B. R. Lawn, and D. B. Marshall, "A Critical Evaluation of Indentation Techniques for Measuring Fracture Toughness: I Direct Crack Measurements," *J. Am. Ceram. Soc.*, **4** [9] 538–53 (1981).
- <sup>20</sup>C. Greskovich and G. E. Gazza, "Hardness of Dense  $\alpha$ - and  $\beta$ -Si<sub>3</sub>N<sub>4</sub> Ceramics," *J. Mater. Sci. Lett.*, **4**, 195–96 (1985).
- <sup>21</sup>R. W. Rice, C. C. Wu, and F. Borchelt, "Hardness-Grain-Size Relations in Ceramics," *J. Am. Ceram. Soc.*, **77** [10] 2539–53 (1994).
- <sup>22</sup>M. J. Hoffman and G. Petzow, "Microstructural Design of Si<sub>3</sub>N<sub>4</sub> Ceramics"; pp. 3–14 in Materials Research Society Symposium Proceedings, Vol. 287, *Silicon Nitride Ceramics—Scientific and Technological Advances*. Edited by I.-W. Chen et al. Materials Research Society, Pittsburgh, PA, 1993.
- <sup>23</sup>L.-L. Wang, T.-Y. Tien, and I.-W. Chen, "Morphology of Silicon Nitride Grown from a Liquid Phase," *J. Am. Ceram. Soc.*, **81** [16] 2677–86 (1998).
- <sup>24</sup>L.-L. Wang, T.-Y. Tien, and I.-W. Chen, "Reply to 'Comment on 'Morphology of Silicon Nitride Grown from a Liquid Phase'," *J. Am. Ceram. Soc.*, **83** [3] 677–78 (2000).
- <sup>25</sup>A. Rosenflanz and I.-W. Chen, "Kinetic of Phase Transformations in SiAlON Ceramics: I. Effects of Cation Size, Composition and Temperature," *J. Eur. Ceram. Soc.*, **19**, 2337–48 (1999). □